DEUTSCHES ELEKTRONEN-SYNCHROTRON DESY

DESY SR-82-18
October 1982

# INVESTIGATION OF CARBON CONTAMINATION OF MIRROR SURFACES EXPOSED TO SYNCHROTRON RADIATION

by

K. Boller, R.-P. Haelbich, H. Hogrefe, W. Jark and C. Kunz

*II. Institut für Experimentalphysik, Universität Hamburg*

*and*

*HASYLAB at Deutsches Elektronen-Synchrotron DESY, Hamburg*

NOTKESTRASSE 85 · 2 HAMBURG 52

DESY SR-82-18
October 1982

# INVESTIGATION OF CARBON CONTAMINATION OF MIRROR SURFACES EXPOSED TO SYNCHROTRON RADIATION

K. Boller, R.-P. Haelbich, H. Hogrefe, W. Jark and C. Kunz

II. Institut für Experimentalphysik, Universität Hamburg
2000 Hamburg 50 and HASYLAB at DESY, 2000 Hamburg 52, FRG

## Abstract

In a systematic investigation gold coated silicon substrates were irradiated with filtered and unfiltered synchrotron radiation under varying conditions. The thickness of the contaminant was measured with a VUV reflectometer through the observation of interference structures. In addition the overall photocurrent which varies with the thickness of the contaminant could be measured. All results show that the cracking process is caused predominantly by the photoelectrons emitted and not by the primary photons. This is specifically supported by the observation of two different growth rates: an initial fast rate up to about 50 Å thickness due to the high photoyield of gold and an asymptotic growth rate of about 10 % the initial rate due to the much smaller yield of carbon. A rate equation deduced from a simple model describes the dependence of the growth rate on residual gas pressure and temperature in good qualitative agreement with the experimental results.

---

to be published in: Proceedings of the International Conference on X-Ray and VUV Synchrotron Radiation Instrumentation, Hamburg, August 1982, Nucl. Instr. & Methods in Physics Research.

## 1. Introduction

The monochromatization of synchrotron radiation in vacuum ultraviolet spectrometers and in advanced x-ray beam lines involves one or several reflections from mirrors and gratings. Carbon contamination of the surfaces is the main reason for severe losses in the efficiency of these elements. While sometimes great efforts are made to increase the angular acceptance of such instruments by factors in the order of two to three, losses of efficiency due to the build-up of carbon layers by one to two orders of magnitude have been reported. The losses are especially severe at and above the carbon K-edge at 280 eV photon energy.

Almost no systematic investigations on this topic have been carried out so far. Nobody appears yet to have studied the build-up of carbon layers under controlled conditions. Inspecting the optical elements shows the areas exposed to synchrotron radiation to be brown from the contamination with a carbonaceous material. In serious cases the carbon film separates from the substrate due to internal stress and comes off in flakes. SHIRLEY1) showed that the absorption behaviour (using reflection EXAFS) of the contamination-overlayer would satisfactorily be explained with an overlayer graphitic in nature. This result was derived from the change of transmission of the grasshopper monochromator2,3) that operates with optical elements coated with platinum. This metal is known to be a good catalyst and it was proposed1) therefore that gold as an inert material should show reduced contamination. This assumption appears to be hard to follow however, since only the first atomic layer is in direct contact with the substrate, while typically between five and several hundred layers are needed to obstruct the reflectivity.

Another important question was raised, however, in this paper[1] namely whether

a) cracking is caused directly by the photons or

b) indirectly through the photoelectons emitted from the substrate.

Suggestions how to reduce or eliminate the contamination are based on common sense. The main ones are to keep the optical elements in a better vacuum, especially the first mirrors in a beam line since it is expected that the contamination rate is both proportional to the partial pressure of hydrocarbons and to the flux of incoming photons. Further the heating of optical elements should reduce the adsorption rate of hydrocarbons. The most expensive and time consuming remedy is practiced in all laboratories: frequent renewal of the optical elements. A nonmechanical cleaning procedure of gratings (glow discharge in an oxygen atmosphere) was recently reported[4]. Its effect on the roughness of the surface is not yet clarified.

In order to obtain a better understanding of the contamination process it was our aim to determine the thickness of the contaminant as a function of exposure time, residual gas pressure and substrate temperature. Simultaneously we wanted to correlate the photoelectron current from the exposed area with the growth of the films. We also tried to vary the kind of hydrocarbon in the system. Although not all experiments were successful and although the phenomena proved to be more complicated than anticipated we could obtain a good first insight into the growth mechanism.

## 2. Experimental Set-Up

The exposures of the mirrors were performed at two beamlines of the electron storage ring DORIS with different spectral compositions of the radiation. In the first beam line (called "IFT") the mirrors were directly irradiated with the "white" synchrotron radiation spectrum at a distance of 27 m from the source point. (At beam line IFT an irradiation through a Kapton filter (7.5 µm) which shows an absorption behaviour almost identical to that of carbon[5] was also possible.) The second station was at the G1-beamline of HASYLAB 15.5 m from the source point, which is a beam deflected by a Kanigen-coated mirror at a grazing angle of 2°. This reflection cuts off all radiation with photon energies above ∿ 1000 eV. Below this energy the reflectivity is near to one so that the spectra of the two beamlines are almost identical up to this energy. The differences are in the contribution of photons with energies above 1000 eV to the contamination process. Due to the large number of photons with energies above 1000 eV in beamline IFT considerable power is deposited on the sample causing a temperature increase during exposure. Because we found it very difficult to control this heating, which has a remarkable effect on the contamination rate, most of the measurements presented in this paper were carried out at beam line G1.

The samples were polished silicon wafers of thickness 0.5 mm covered with an evaporated layer of 700 Å Au. They were clamped onto a temperature controlled copper block and were illuminated at an approximately 1 cm wide spot. The conditions of illumination are given in table 1.

The thickness of the contaminant was obtained from the interference structures in the reflectivity spectra. The reflectivities of contaminated and clean gold mirrors were measured with a VUV reflectometer (mounted also at the beam line GI)for an angle of incidence $\alpha = 60^0$ as a function of the wavelength of the incident light ($50\ Å \leq \lambda \leq 500\ Å$). The ratio of both spectra shows a modulation caused by the carbonaceous overlayer (see Fig. 1). These measured curves were fitted with theoretical calculations based on the formula derived by PEPPER[6)] and using the optical constants for C and Au given by HAGEMANN et al.[7)]. Fitting parameter was the film thickness d. Thus it was possible to determine contamination thicknesses in the range 50 Å to 300 Å. It would have been desirable to be able to determine the thickness of even thinner films but the interference structures of such films occur at wavelengths where C and Au have too low a reflectivity for angles of incidence less than $60^0$. For more grazing angles, however, the structures occur outside the range of our monochromator.

In addition we could measure in some cases the photoyield during the exposure with a ring anode facing the exposed area of the mirrors. The following parameters could be varied during the experiment: sample temperature, residual gas pressure, kind of gas. In one experiment Au was replaced by CsI.

## 3. Results and Discussion

### 3.1 Pressure dependence

The first experiments were concerned with irradiating the samples under different vacuum conditions by varying the pump down time of the system before irradiation. About $10^{-7}$ Torr was the lowest pressure obtainable in beam line GI and $10^{-5}$ Torr in beam line IFT (see table 1). The intention was to reduce the contamination rate due to the residual hydrocarbons to such an extent that a well defined addition of specific gases would give the dominant contaminating effects. Fig. 2 shows the astonishing result that the thickness obtained with the same dose is almost independent of pressure. The points denoted by squares and triangles are obtained under the conditions of the IFT-beamline which give a higher effective dose since the spectrum of synchrotron radiation is not filtered by a mirror there (the "dose" is obtained by electron current multiplied by exposure time). Therefore for those points only the trend for the two squares or the two triangles (each group belonging to a series with other parameters kept fixed) is meaningful.

Under these circumstances it is not surprising that the addition of methane gave practically no effect (in one case starting from a base pressure of $\sim 2 \cdot 10^{-5}$ Torr $9 \cdot 10^{-5}$ and $4 \cdot 10^{-4}$ Torr was admitted). The addition of a more complicated organic compound ($C_3H_8CO$) up to $6 \cdot 10^{-4}$ Torr appeared to give a small effect, but no systematic variation of the pressure of this gas was performed. Altogether, the effects are much less pronounced than expected from a simple proportionality to the pressure and it appears clear from these experiments that a much better base vacuum is needed if pressure effects and effects of specific gases should be studied.

We can understand our results from the following simplified model. The processes shown in Fig. 3 allow us to set up a rate equation if we assume that one monolayer of hydrocarbons can be adsorbed and that at the location where one molecule on the surface is cracked by either a photon or an electron a new free place for adsorption is created. The rate equation is given by

$$dN/dt = S - R - V - K. \qquad (1)$$

Here N is the density of crackable molecules on the surface, S is the rate of gas flow to the surface, R the rate of reflected molecules, V the rate of reevaporated molecules and K the rate of cracking of molecules on the surface. A once cracked molecule is assumed to be pinned to the surface. If $n = N/N_{max}$ is the fraction of filled places, and if we assume that only those molecules are reflected which hit a filled place then $R = n\,S = \text{const} \cdot nP$, since S is proportional to the pressure P. Further $K = \text{const} \cdot n \cdot I$ where I is the current density of either photons or photoelectrons. The reevaporation rate is $V \propto nTe^{-\Delta E/kT}$ (the temperature dependence could also be more complicated). The steady state solution of (1) is obtained by setting $dN/dt = 0$ yielding for the contamination rate

$$K = C_1 \frac{P\,I}{C_2 P + C_3 T e^{-\Delta E/kT} + I}\,, \qquad (2)$$

where the $C_i$'s are constants.

Figure 4 shows the contamination rate K as a function of the intensity I (which is the photoelectron current as we shall prove later). The constants are chosen appropriately in order to give a dependence on pressure in qualitative agreement with our results. The parameter temperature was kept fixed here. It is interesting to note from Fig. 4 that at high pressures (here above $10^{-7}$ Torr) the contamination rate is practically independent of pressure as observed in Fig. 2. In the rate equation (2) this is borne out as a dominance of the first term in the denominator. In the microscopic picture of Fig. 3 an empty place on the surface is filled much faster than the rate at which photoelectrons arrive, thus practically all positions available for contaminants are filled all the time.

A complementary process would be intensity saturation that is at very high intensities and sufficiently low pressure the contamination rate becomes independent of intensity, namely the surface is almost empty and each hydrocarbon molecule is cracked immediately (see Fig. 4 and equation (2)).

Finally, if in equation (2) the second term in the denominator dominates (i.e. at low pressure, low intensity and high temperature) only then the naively expected proportionality to both P and I emerges. This can be also seen in Fig. 4.

### 3.2 Dose dependence

In another series of experiments we measured the thickness of the contaminant as a function of the dose applied. If the cracking of hydrocarbons was induced by the photons directly the thickness should grow proportional to the dose. The result of such measurements is shown in Fig. 5. Although films with thicknesses under ~ 50 Å could not be measured the zero point by definition is another valid point in the diagramme. The interpolated curve suggests that two different growth rates are involved, one initial fast rate which dominates up to a thickness of 50 to 100 Å and a much slower asymptotic rate. The fast rate is at least a factor of 5 (in some cases a factor of 10) larger than the asymptotic rate. This is, however, only a lower limit since no data points are available below 50 Å.

Such a thickness dependent growth rate is in contradiction to a direct photoinduced cracking process while it fits well to photoelectron induced cracking. Initially the photoyield of pure gold determines the electron current penetrating the surface. While the carbon film grows, less and less photoelectrons excited in the Au substrate are able to reach the surface and ultimately only electrons excited in the carbon layer are emitted. Since the photoelectric yield of C is much less than that of Au (see below) it is reasonable that the contamination rate is decreasing continuously and saturates at a value determined by the yield of C (in whichever modification it may grow).

Another important test for checking the assumption of a direct photoncracking was made the following way: two films were contaminated in the IFT beam with equal dose (mA x sec.). In one of the illuminations, however, a 7.5 μm thick Kapton film was inserted into the path of the beam. Since such a film[5)] is filtering out completely that band of radiation which is preferentially absorbed by all hydrocarbons the contamination process should be reduced by orders of magnitude. The observation gave, however, practically the same thickness in both cases what we consider to be a strong argument against primary photocracking.

The third type of experiments on this question was a direct correlation of the contamination with the measured photocurrent. This will be described in section 3.3.

We shall now work out a model for the number of photoelectrons with an energy high enough to crack hydrocarbons on the surface as a function of the carbon thickness d (see Fig. 6). In this calculation we follow closely the model of yield spectroscopy[8)] and extend it to a two layer system. While all those electrons contribute to the photoelectric yield which have a kinetic energy high enough to penetrate the surface barrier only those can crack an adsorbed hydrocarbon molecule which have a kinetic energy $E_{kin}$ in vacuum above a certain threshold. We estimate this threshold energy to be roughly 5 eV (about 10 eV relative to the Fermi energy). More specifically an energy dependent cross section for this process should be considered, which is unknown since we even do not know exactly which species of hydrocarbon is involved. Further, this cross section is dependent on the substrate on which the process takes place.

In a certain simplification we assume that we can define an average quantity, the mean escape depth $\ell_C$ and $\ell_{Au}$ of chemically active electrons. Figure 6 visualizes that this length is to be taken from the cross where the primary photoexcitation takes place to the point where the electron finally stops projected on the normal to the surface. On its path several multiplication processes will occur in conjunction with a loss in energy. If we follow now the general assumption of a material independent "universal curve"[9)] for the mean free path of monoenergetic electrons (the distance between the scattering processes in Fig. 6 if phonon scattering is neglected) then we can assume $\ell_C = \ell_{Au} = \ell$. Of course $\ell(h\nu)$ is a weak function of the energy $h\nu$ deposited in the process.

Since $\mu_{Au}$ and $\mu_C$, the photon absorption coefficients are typically much smaller than $^1/\ell$ we obtain the probability for a primary excitation in a layer of thickness $\Delta x$ as $\Delta x \cdot \mu_i$ ($i$ = Au,C). Since practically all the deposited energy $h\nu$ is transformed into electron excitation (direct emission, scattering, Auger etc.) it is reasonable to assume that a multiplication factor $M(h\nu) \propto h\nu/E$ comes into play, where E is the energy at which the cross section for cracking has its center of gravity or its highest value if it happens to be peaked. E is measured relative to the Fermi energy. The multiplication probability of a primary fast electron is obviously reduced if it originates in the topmost layers. Neglecting this, is another approximation we make. Under these simplifying assumptions the flux of chemically active photoelectrons $\Delta I_e$ penetrating the top surface due to all primary processes originating in a layer of thickness $\Delta x$ at depth x is (with $I_o$ the photon intensity) given by

$$\Delta I_e \propto I_o(h\nu)(h\nu/E)\ \mu_i\ e^{-\frac{x}{\ell}}\ \Delta x d\nu \tag{3}$$

Integrating over x and $\nu$ gives

$$I_e \propto \int d\nu\ I_o(h\nu)(h\nu/E)\ \ell\ \left[\mu_{Au} e^{-d/\ell} + \mu_C(1-e^{-d/\ell})\right] \tag{4}$$

We make now a rough estimate for the parameters involved and try to fit experimental curves with the following equation

$$K = c' I_e = c''\left[\frac{\langle\mu_{Au}\rangle}{\langle\mu_C\rangle}\, e^{-d/\bar{\ell}} + (1-e^{-d/\bar{\ell}})\right] \tag{5}$$

where c' and c'' are constants. Setting $K = c' I_e$ is justified from (2) since we are in the limit of pressure saturation.

A rough estimate was made for $\ell(h\nu)$ with E = 10 eV using a random walk model and assuming that each electron scattering process in Fig. 6 leads to an equal distribution of energy to both electrons. With the help of the "universal curve"[9)] we obtain: $\ell$ = 23 Å for $h\nu$ = 100 eV, $\ell$ = 35 Å for $h\nu$ = 1000 eV and $\ell$ = 65 Å for $h\nu$ = 5000 eV. This is in good general agreement with the value of ∿ 50 Å for the thickness at which the transition from a fast to a slow contamination occurs in Fig. 5. Further

$$\langle\mu_i\rangle = \int_{10eV}^{h\nu_{max}} d\nu \quad \mu_i \quad I_o(h\nu)(h\nu/E) \Big/ \int_{10eV}^{h\nu_{max}} d\nu\ I_o(h\nu)(h\nu/E) \tag{6}$$

is calculated with the tables for $\mu_i$ 7) and the spectrum of synchrotron radiation $I_0(h\nu)$. In setting up this integral the weak dependence of $\ell$ on $h\nu$ was suppressed. With $h\nu_{max}$ = 1000 eV for the G1 beam line we obtain $\langle\mu_{Au}\rangle/\langle\mu_C\rangle \sim 10$ from (6). This is in astonishing good agreement with the order of magnitude difference between the two growth rates in Fig. 5. An actual fit according to (5) of measurements on beam line G1 is shown in Fig. 7. Within the limitations of all the approximations made no better agreement could be expected. Of course the missing measurements for thicknesses below ∿ 50 Å makes it difficult to draw more than qualitative conclusions from such a fit.

### 3.3 Measurements of the photocurrent

Measurements of the photoelectric yield as a function of dose are shown in Fig. 8. We have to be aware that the overall yield as measured here is not identical to the yield of chemically active electrons causing the build up of the carbon layer. Especially the escape depth of the slower electrons which could dominate the yield and are included here is larger. The obvious faster contamination on a CsI substrate of 200 - 300 Å thickness (Fig. 8) should therefore be considered qualitatively rather than quantitatively as a consequence of the higher photoelectric yield of CsI

compared to that of Au 10).

In an expanded time scale we have observed also the behaviour of the photoyield at the beginning of the exposure of a fresh gold substrate. Fig. 9 gives a typical result. Initially at point 2 a peak occurs which disappears in a very short time. This could be tentatively identified with a work function change when the first adsorbed layer is cracked (such peaks occur whenever the illumination of the sample is interrupted for some time, it was proven that it is no artefact of the electronics). Then between points 3 and 4 there is a slight rise in the intensity by a few percent of the overal intensity. After point 4 the intensity falls off ultimately with an exponential decay as shown in Fig. 8.

This initial rise is not included in our model leading to equation (5). As mentioned already above our model does not include the fact that the electrons originating from a primary absorption in the topmost layers can escape with high probability without undergoing the multiplication cascade. Due to this they contribute less to the yield. The carbon layer building up on the Au surface can therefore have two competing effects, one is the absorption of slow electrons, the other is the multiplication. Assuming the existence of small differences in the scattering processes in Au and C (which we had neglected in deriving (5)) we could imagine that the balance of these two effects is more in favor of multiplication in C. In other words we use the first layers of C here as a secondary emission multiplier.

It is interesting now to attempt a correlation between this effect and the thickness of the carbon layer. In Fig. 10 we have plotted the decrease of the yield at the end of an exposure against the measured C thickness. An extrapolation to 100 % yield suggests that we should correlate a C thickness of 50 Å with the maximum at point 4 in Fig. 9.

### 3.4 Temperature dependence of contamination

Making use of the results from section 3.3 we have measured the photoelectric yield as a function of temperature as shown in Fig. 11. There is a striking dependence of the yield variation on temperature. By plotting the dose at the photocurrent maximum (Fig. 9) as a function of temperature we obtain the curve shown in Fig. 12 which essentially is the inverse of the contamination rate K as a function of temperature. It is clearly borne out that an increase of the temperature by 100 degrees can reduce K by a factor of 5.

## 4. Conclusion

We could show that the carbon contamination on mirrors exposed to synchrotron radiation can consistently be explained as a cracking of hydrocarbon molecules by photoelectrons from the substrate and from the contamination layer itself. A fast initial growth determined by the photoyield of Au is followed by an approximately ten times slower growth rate determined by the yield of carbon (or a carbonaceous material) above 50 Å. It is not clear how to exploit this insight technically in order to reduce contamination without reducing the reflected band width at the same time.

The growth process as a function of pressure, temperature and electron current density can be described by a rate equation. This equation explains e.g. that under certain photon flux conditions, as encountered at DORIS, a variation of the pressure between $10^{-7}$ and $10^{-4}$ torr has almost no influence on the growth rate ("pressure saturation").

Increase of the temperature by 100° above room temperature can reduce the growth rate under certain conditions to 20 %.

More quantitative measurements in a well defined hydrocarbon environment are needed for a better understanding of the processes involved. Especially it is desirable to follow the growth process in the thickness range below 60 Å.

The importance of the indirect photochemical reaction mediated through the photoelectrons shown by our experiments may have some consequences also for other photochemical reactions like e.g. photostimulated desorption[11]. At least such experiments have to be seriously checked in this respect.

## Acknowledgements

We wish to thank the Institut für Festkörpertechnologie der Fraunhofergesellschaft, München, for allowing us to use their facilities at DORIS. Further, we thank H. Zeiger for his help in preparing the substrates. This work was supported by the Bundesministerium für Forschung und Technologie.

## References

1. D.A. Shirley, Beam Line Chemistry, Workshop on X-ray Instrumentation for Synchrotron Radiation Research. Editors: H. Winick and G. Brown SSRL Report No. 78/04 May 1978
2. F.C. Brown, R.Z. Bachrach and L. Lien, Nucl. Instr. and Meth. 152 (1978) 73
3. R.Z. Bachrach, S.A. Flodstrom, R.S. Bauer, V. Rehn and V.O. Jones, Nucl. Instr. and Meth. 152 (1978) 135
4. W.R. McKinney and P.Z. Takacs, Nucl. Instr. and Meth. 195 (1982) 371
5. E.T. Arakawa, M.W. Williams, J.C. Ashley and L.R. Painter, J. Appl. Phys. 52 (1981) 3579
6. S.V. Pepper, J. Opt. Soc. Am. 60 (1970) 805
7. H.J. Hagemann, W. Gudat and C. Kunz, J. Opt. Soc. Am. 65 (1975) 742 and DESY Report SR 74/7 May 1974
8. W. Gudat and C. Kunz, Phys. Rev. Lett. 29 (1972) 169
   W. Gudat, Ph.D. Thesis, Hamburg University 1974 and
   DESY Internal Report F41-74/10
9. I. Lindau and W.E. Spicer, J. Electron. Spectrosc. Relat. Phenom. 3 (1974) 409
10. W. Lenth, diploma thesis, Hamburg University 1975 and DESY Internal Report, F41-75/07
11. e.g. M.L. Knotek, V.O. Jones and V. Rehn, Phys. Rev. Lett. 43 (1979) 300
    R. Franchy and D. Menzel, Phys. Rev. Lett 43 (1979) 865

Table 1: Conditions of irradiation at the two different stations

| | Beamline IFT ("white" radiation) | Beamline G1 (reflected beam) |
|---|---|---|
| Storage ring conditions | DORIS<br>R = 12.12 m | |
| Electron energy | 3.3 GeV | 3.3 GeV |
| Electron current | $\leq$ 60 mA | $\leq$ 80 mA |
| Source distance | 27 m | 15.5 m |
| Residual gas pressure | $\geq 2\text{x}10^{-5}$ torr | $\geq 2\text{x}10^{-7}$ torr |
| Mirror temperature | $20^{\circ}$ C | $20^{\circ}\ \mathrm{C} \leq T \leq 140^{\circ}$ C |
| Exposure times | $\leq$ 3000 s | $\leq$ 3000 s |

## Figure captions

Fig. 1 Ratio of the reflectivity of a contaminated to a non contaminated Au coated silicon wafer. The angle of incidence was $60^{\circ}$. The large scale oscillations are fitted by a theoretical two layer model yielding 63 Å for the C film. The small oscillations around 100 Å are due to interferences in the Au film.

Fig. 2 Thickness of the contamination film as a function of pressure, corrected for equal dose. Circles below $10^{-5}$ Torr at beam G1 (1.5 GeV), squares and triangles at beam IFT (3.3 GeV). Triangles and squares were measured under different conditions. The correction to equal conditions is indicated by arrows.

Fig. 3 Build-up of a contamination layer from cracked hydrocarbons. S = flux of incoming hydrocarbons, R = flux of reflected hydrocarbons, K = rate of cracked hydrocarbons, N = adsorption density.

Fig. 4 Contamination rate as a function of photoelectron intensity $I_e$ and pressure P according to equation (2). The constants were chosen in such a way that the pressure saturation starts above $10^{-7}$.

Fig. 5 Thickness of the contamination layer as a function of dose. Curve A at IFT beam (3.3 GeV) $29^{\circ}$C, $1\text{-}2\cdot10^{-5}$ Torr, curve B at G1 beam $25^{\circ}$C, $1\text{-}2\cdot10^{-6}$ Torr.

Fig. 6 Creation (x) and multiplication of photoelectrons on their way to the surface (schematic).

Fig. 7 Fit of measurements as those in Fig. 6 with an integral over K from equation (5). The ratio $\frac{\langle \mu_{Au} \rangle}{\langle \mu_C \rangle}$ was varied.

Fig. 8 Photoelectric yield measured during contamination of a Au and a CsI coated substrate at beamline G1 (1.5 keV) $1.2 \cdot 10^{-5}$ Torr in both cases. Both yield currents are set 100 % at the maximum, a background had to be subtracted.

Fig. 9 The initial behaviour of the photoelectron current as a function of time.

Fig. 10 Correlation between the final thickness and the remaining photoelectron current at the end of an exposure at beam G1 (1.5 GeV) compared to the current at the maximum (point 4 in Fig. 9) ($1.2 \cdot 10^{-6}$ - $1.9 \cdot 10^{-7}$ Torr, 25 - 140°C).

Fig. 11 Photoyield as a function of dose for different temperatures at beam G1 (1.5 GeV), $1.2 \cdot 10^{-6}$ - $1.5 \cdot 10^{-7}$ Torr.

Fig. 12 Dose at which the maximum (point 4 in Fig. 9) which we identify with 50 Å thickness is reached as a function of temperature. Measurements were taken at beam G1 (1.5 GeV). Since the pressure varied from $1.2 \cdot 10^{-6}$ to $1.9 \cdot 10^{-7}$ Torr and other conditions also changed the interpolation curve is connecting points obtained with almost equal conditions.

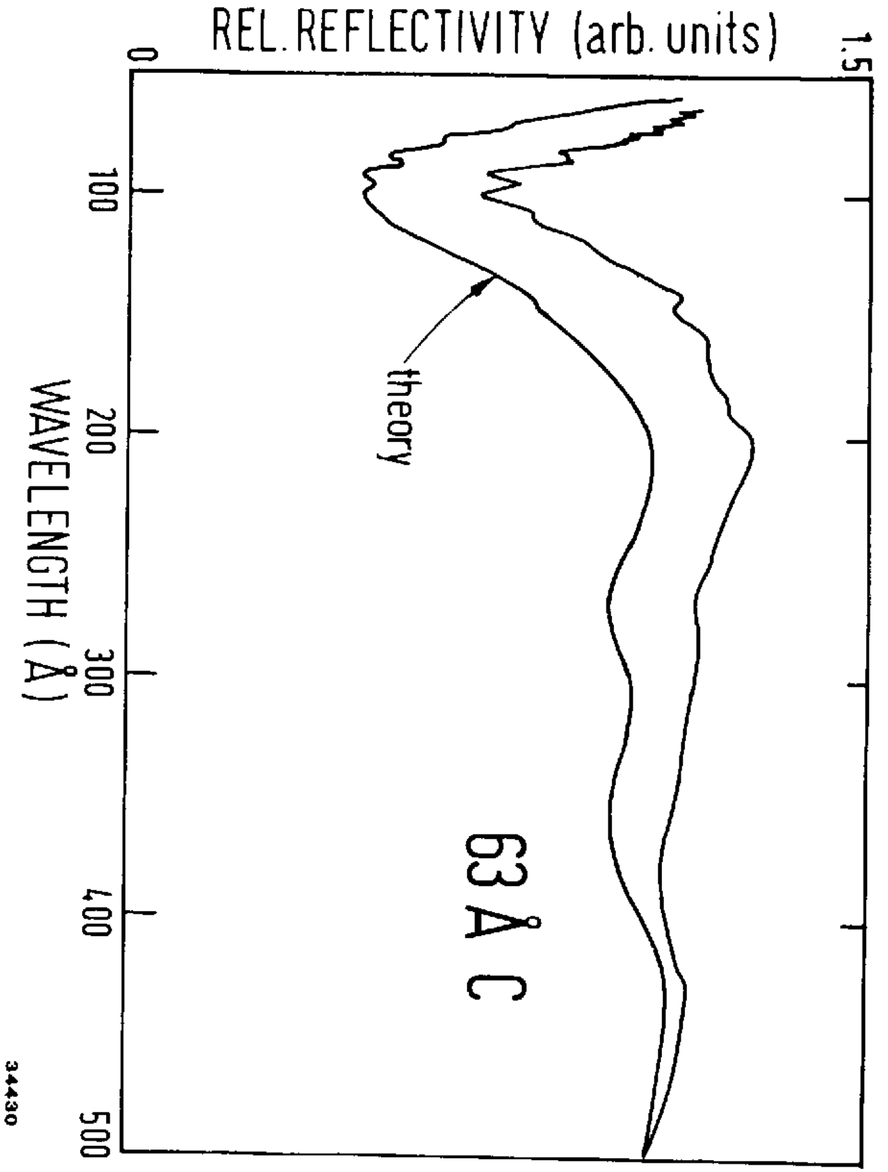

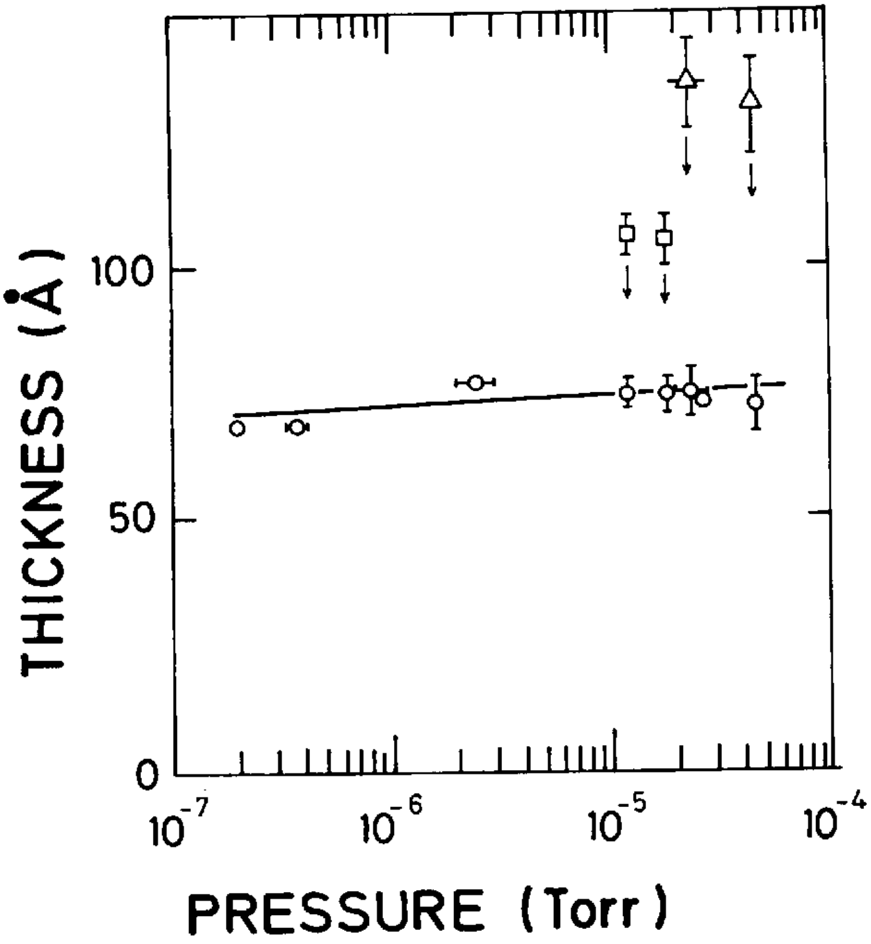

THICKNESS (Å)
100
50
0
$10^{-7}$
$10^{-6}$
$10^{-5}$
$10^{-4}$
PRESSURE (Torr)

Fig. 2

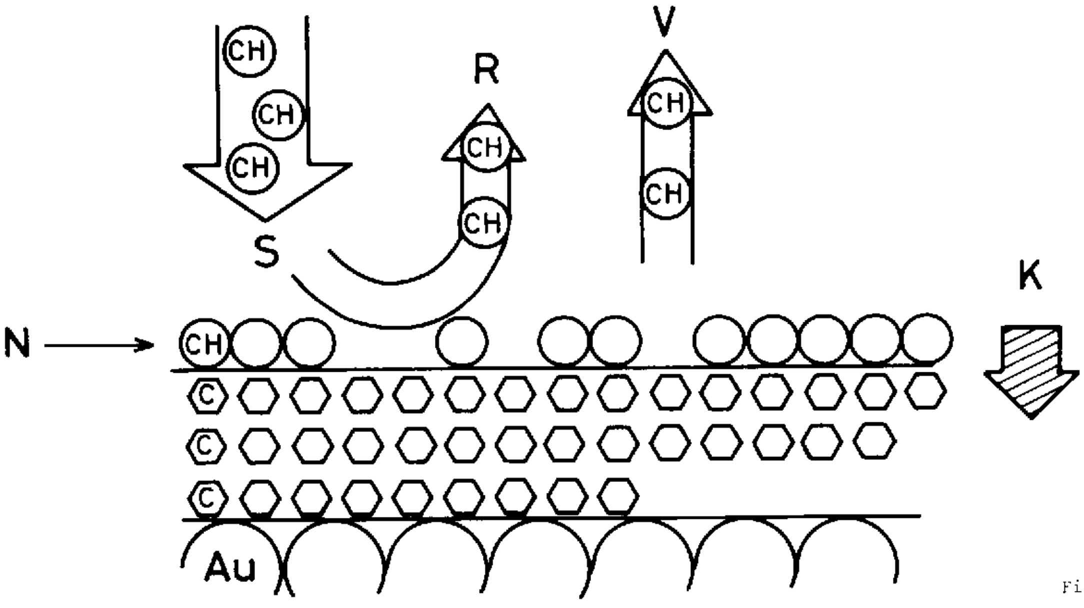

CH
S
R
V
K
N
C
Au

Fig. 3

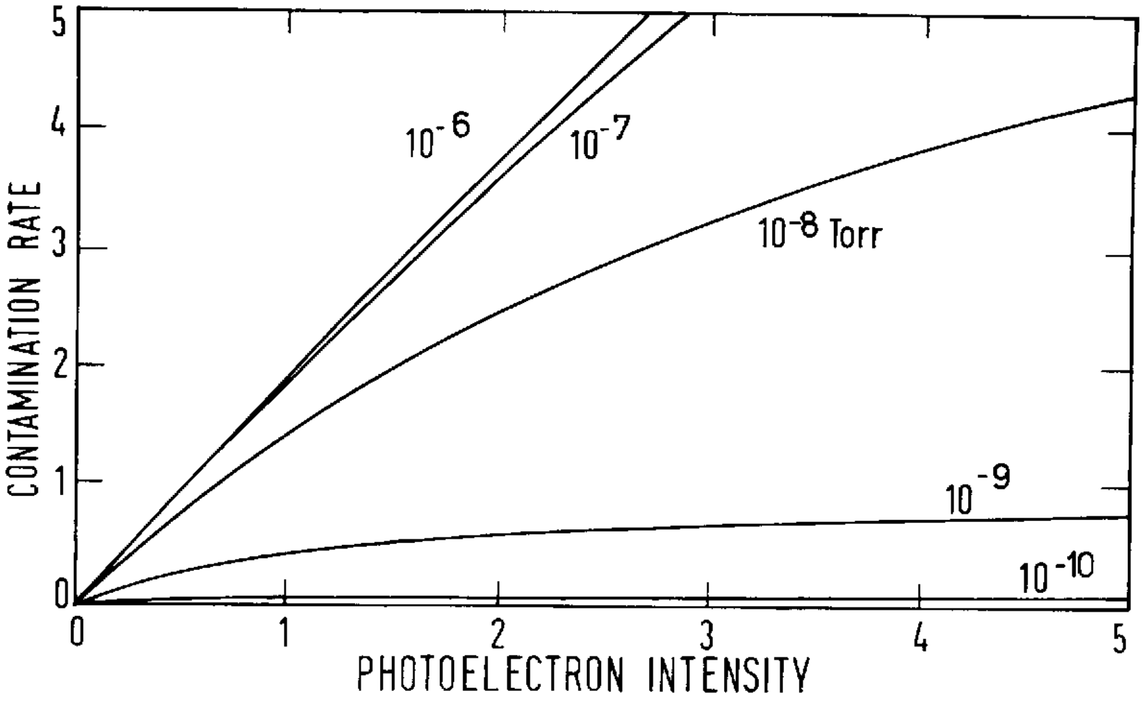
CONTAMINATION RATE
0
1
2
3
4
5
PHOTOELECTRON INTENSITY
0
1
2
3
4
5
$10^{-6}$
$10^{-7}$
$10^{-8}$ Torr
$10^{-9}$
$10^{-10}$

Fig. 4

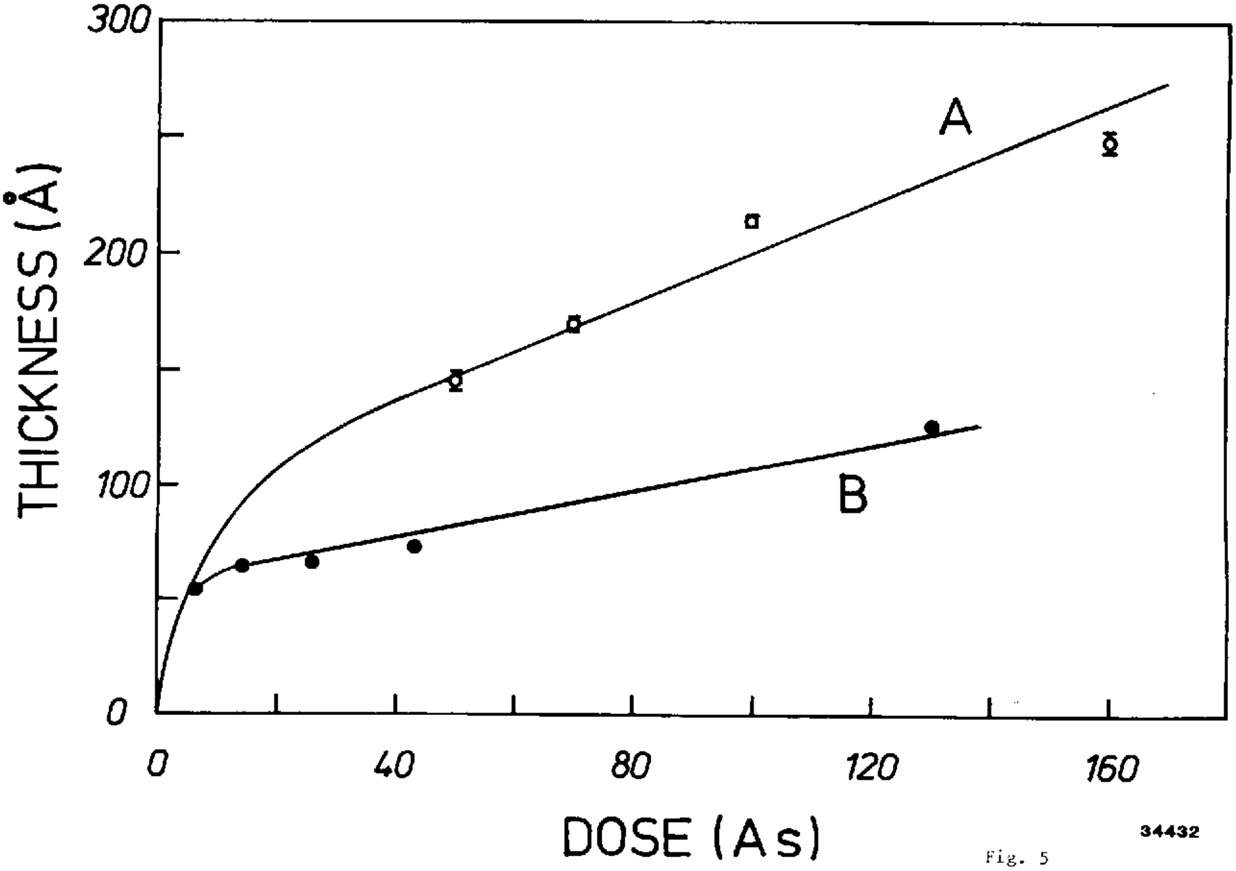
THICKNESS (Å)
0
100
200
300
DOSE (As)
0
40
80
120
160
A
B
34432

Fig. 5

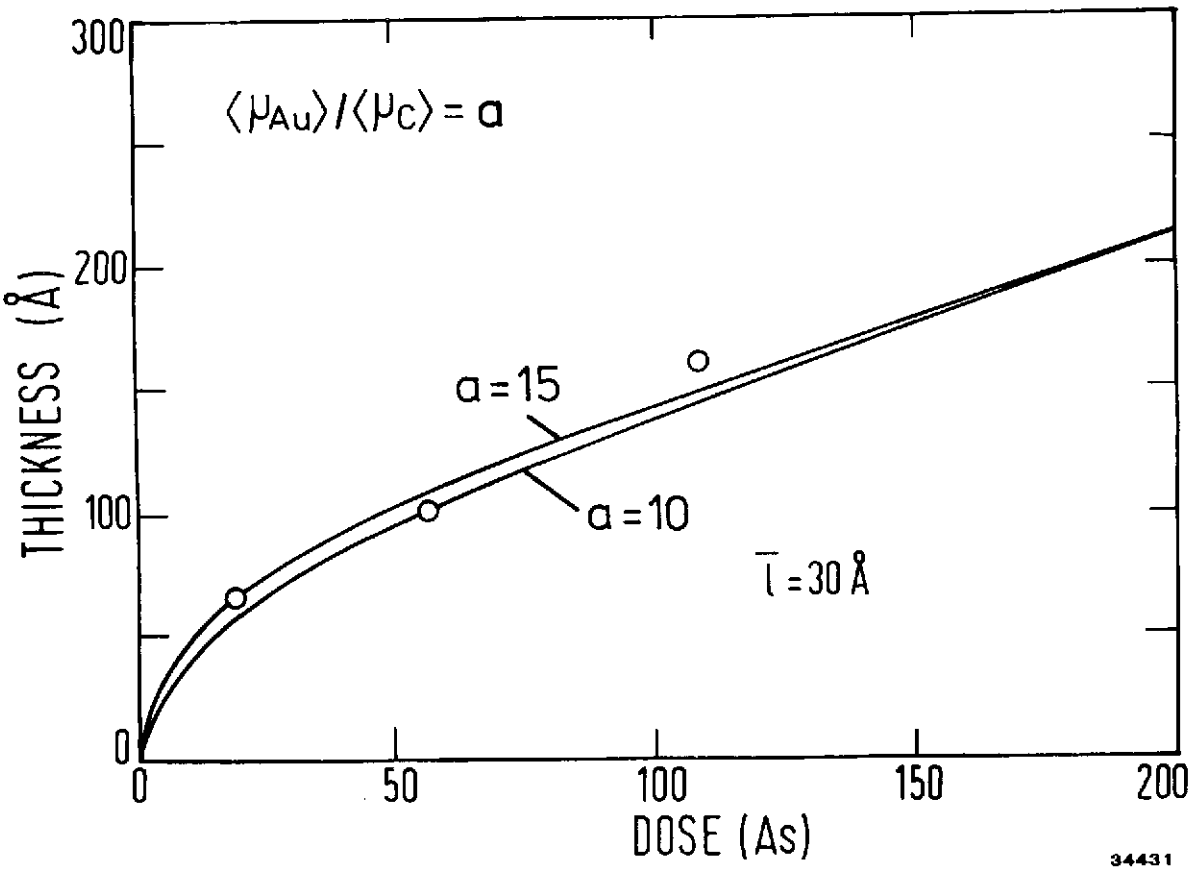

300
200
100
0
THICKNESS (Å)
$\langle \mu_{Au} \rangle / \langle \mu_C \rangle = a$
a = 15
a = 10
$\bar{l}$ = 30 Å
0
50
100
150
200
DOSE (As)
34431

Fig. 7

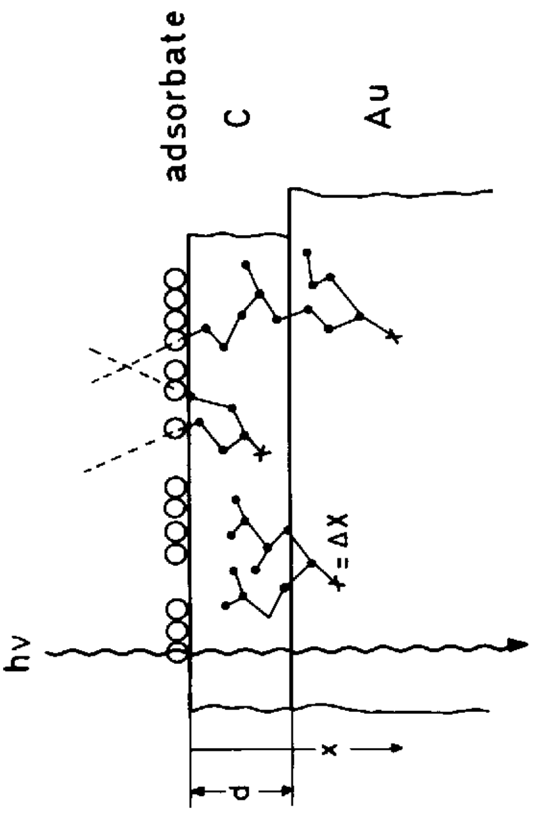

adsorbate
C
Au
hν
= Δx
x
d

Fig. 6

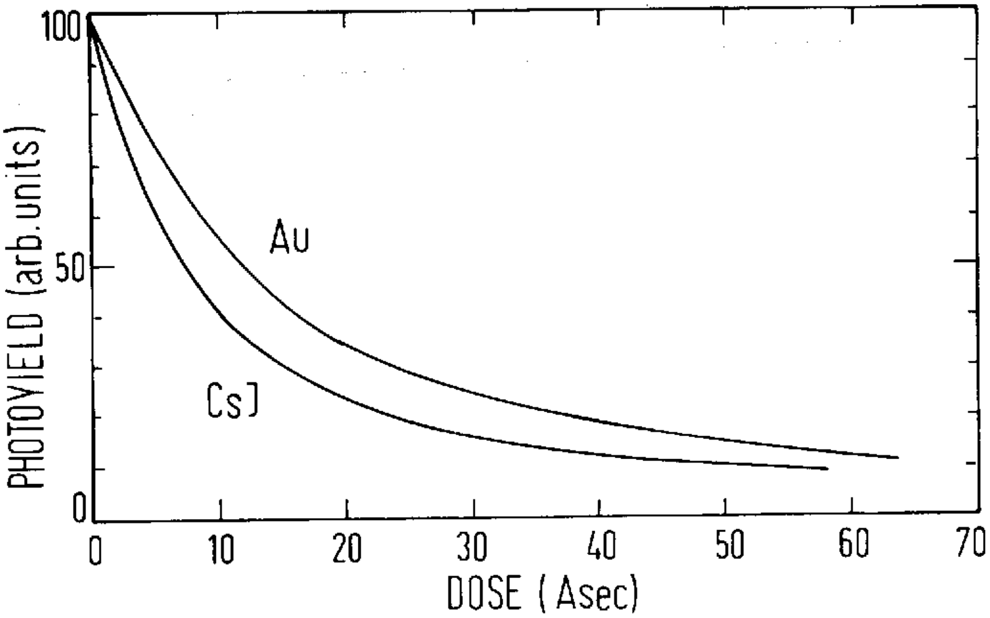

PHOTOYIELD (arb.units)
100
50
0
Au
Cs]
0
10
20
30
40
50
60
70
DOSE (Asec)

Fig. 8

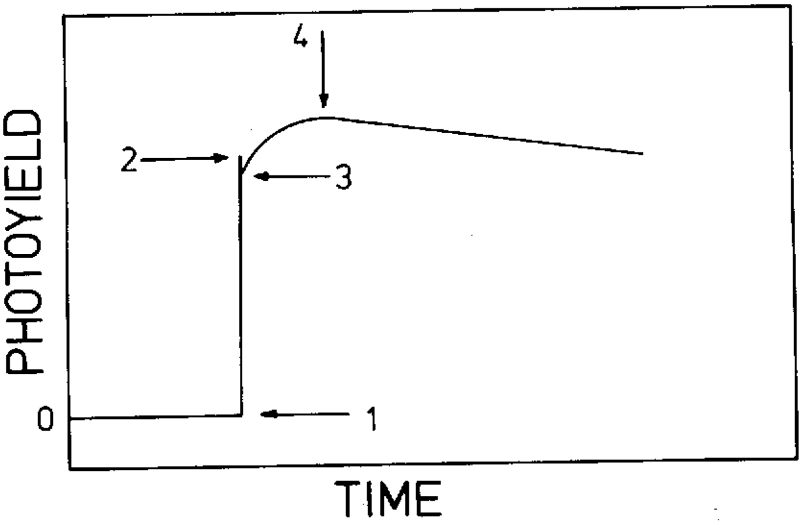

PHOTOYIELD
0
4
2
3
1
TIME

Fig. 9

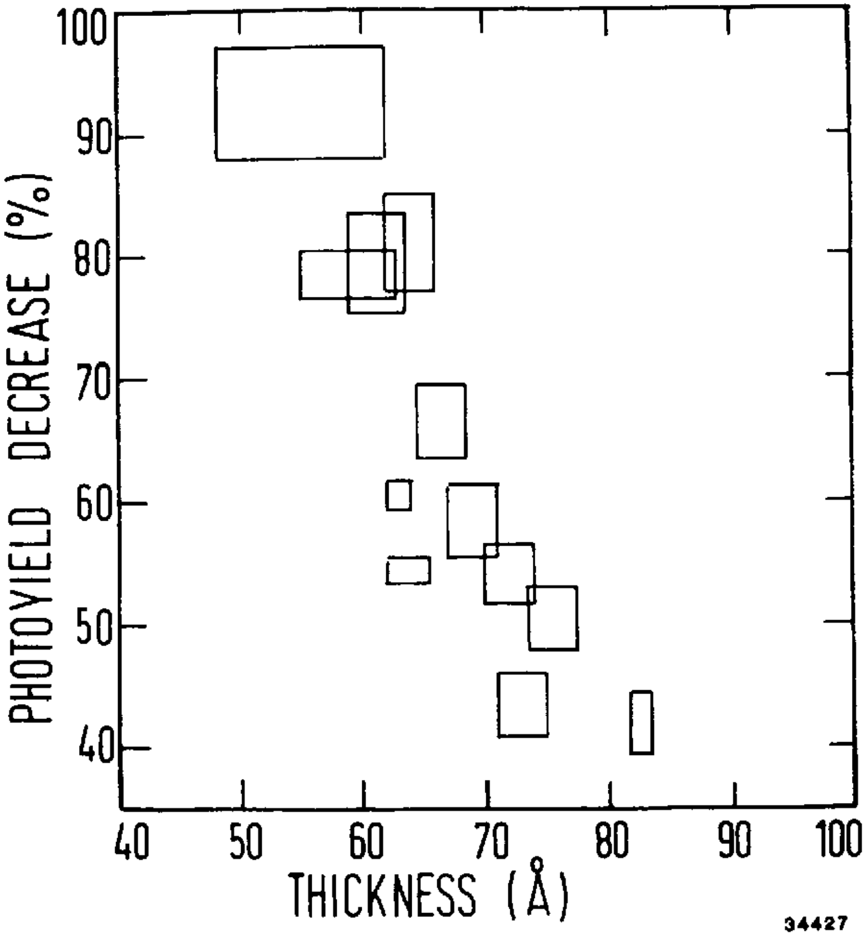
PHOTOYIELD DECREASE (%)
100
90
80
70
60
50
40
THICKNESS (Å)
40
50
60
70
80
90
100
34427

Fig. 10

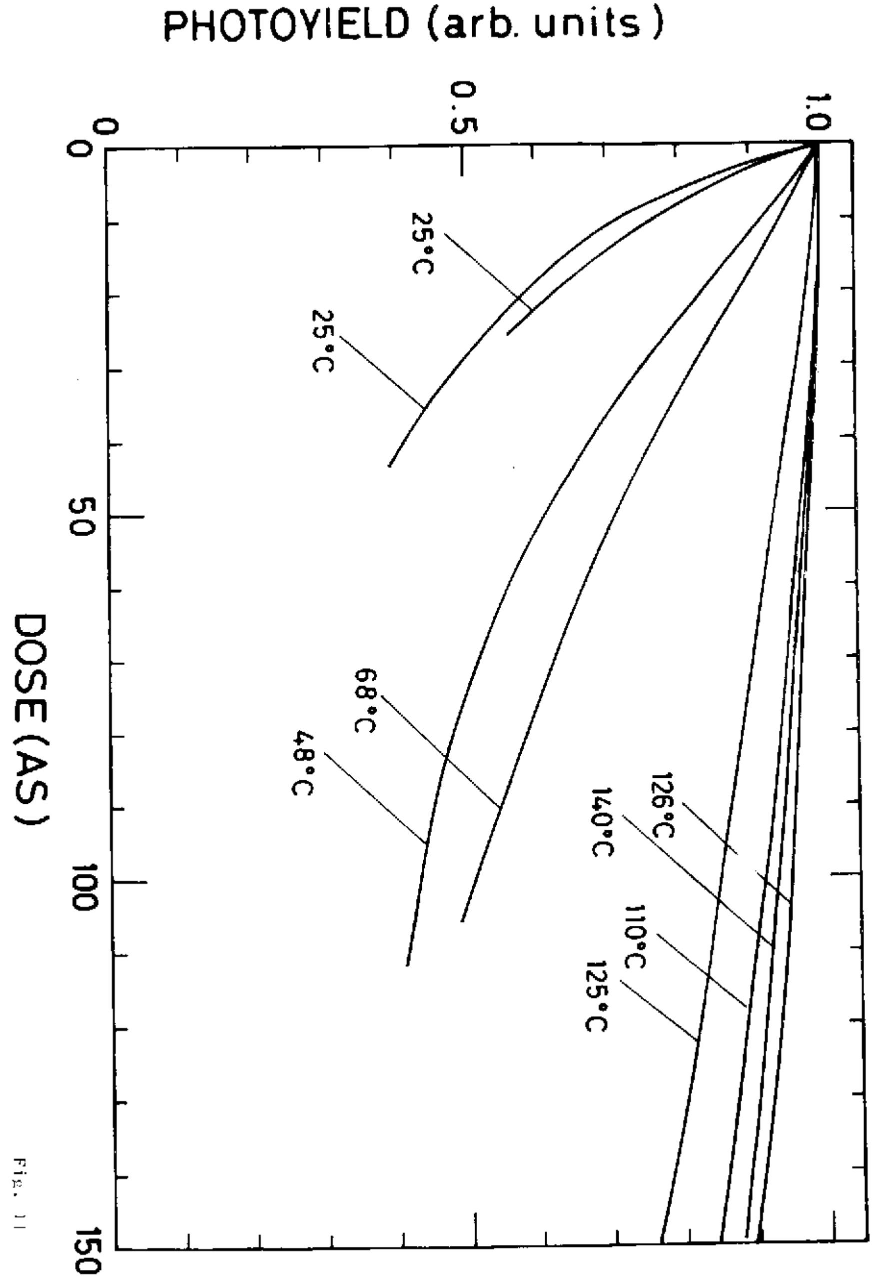
PHOTOYIELD (arb. units)
0
0.5
1.0
DOSE (AS)
0
50
100
150
25°C
25°C
68°C
48°C
126°C
140°C
110°C
125°C

Fig. 11

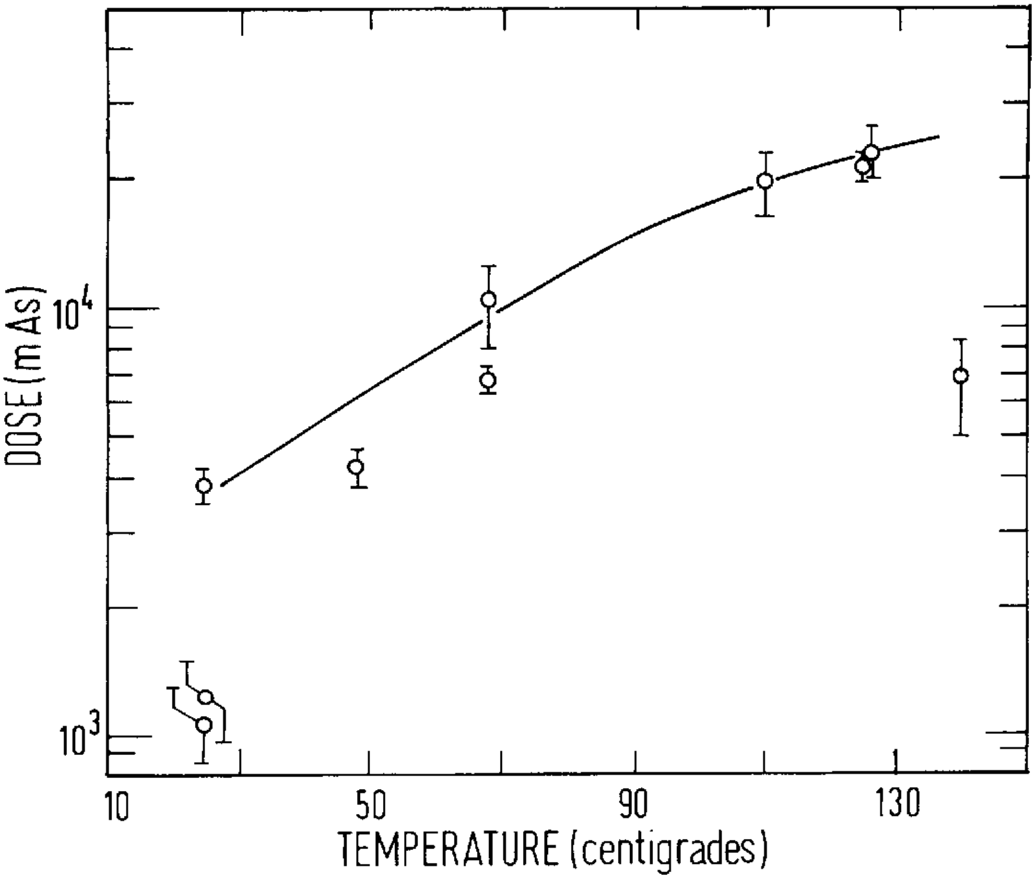

Fig. 12